PERGAMON

International Journal of Solids and Structures 36 (1999) 3257–3275

INTERNATIONAL JOURNAL OF SOLIDS and STRUCTURES

Dynamic plastic behavior of circular plate using unified yield criterion

Guowei Ma, Shoji Iwasaki, Yutaka Miyamoto*, Hideaki Deto

Department of Civil and Environmental Engineering, Iwate University, 020, Morioka, Japan

Received 12 November 1996; in revised form 26 March 1998

Abstract

Dynamic plastic behavior of a rigid-plastic simply supported circular plate under moderate partial uniformly distributed impulsive load is complemented by using a unified yield criterion which consists of a generic of convex piecewise linear yield criteria. Upper bound and lower bound plastic responses of the plate under rectangular pulse are obtained; response behavior of the plate with respect to the Mises criterion is derived by a proximal manner. The inconstant circumferential moment distribution and the non-linear flow velocity distribution in the periods corresponding to the two motion phases are suggested in this paper. Static and kinematic admissibility of the dynamic plastic solutions is discussed and two types of moment profiles for the plates under intense dynamic load are supposed for studying in the future.

Nomenclature

$\sigma_1, \sigma_2, \sigma_3, \sigma_0$	principal stresses and uniaxial tensile strength
$\tau_{13}, \tau_{12}, \tau_{23}$	principal shear stresses
b	weighting coefficient in the unified yield criterion
a_i, b_i $(i = 1, 2)$	coefficients in the unified yield criterion
M_r, M_θ, M_0	radial bending moment, circumferential bending moment and ultimate bending moment
Q_r, P	transverse shear force and rectangular impulsive load
τ, T, t	duration of pulse, duration of and actual response time, respectively
$\tilde{\mu}$	mass per unit area
R, a	radius variable and radius of circular plate
$\dot{k}_r, \dot{k}_\theta$	dimensionless radial and circumferential curvature rates
$c_{1i}, c_{2i}, c_{3i}, c_{4i}$ $(i = 1, 4)$	integral constants of velocity fields and moment fields

* Corresponding author. Fax: 0081 19 621 6460; E-mail: miyamoto@iwate-u.ac.jp

PII: S0020–7683(98)00130–9

r_p, r_1, r_2, r_s	dimensionless loading radius, dividing radius of the first phase of motion, the second phase of motion and the static plastic limit state
p_0, p_s, p_d	dimensionless impulsive load, static plastic limit load and maximum statically admissible impulsive load
η	response delaying factor
W, W_f	actual displacement response of the plate, permanently deformed transverse displacements at the plate center
$\dot{w}_1, \ddot{w}_1, \dot{w}_2, \ddot{w}_2$	dimensionless velocity and acceleration responses of the two motion phases
α, α_d	statically admissible loading factor and maximum admissible loading factor
k_e	kinetic energy absorbed during the first phase of motion

Dimensionless variables
$r = R/a$, $m_r = M_r/M_0$, $m_\theta = M_\theta/M_0$, $p = Pa^2/M_0$, $q = Q_r a^2/M_0$, $\mu = \tilde{\mu}a^3/M_0$, $w = W/a$.

1. Introduction

Static deformation of elasto-plastic structures applies only if the loading magnitude is less than the plastic collapse force. With impact or explosive blast loading, however the structures can be subjected to an intense but short duration pressure or force pulse that exceeds the plastic collapse force. The dynamic plastic behavior of beams is investigated sufficiently in the past (Stronge and Yu, 1993), however, there are some difficulties to get the analytical solution for plate and shell in dynamic plastic deformation state because of the complicated constitutive model. Circular plates as special structures are always examined by analytical method for their axisymmetric characteristics. Exact theoretical solutions to dynamic response of a rigid, perfectly plastic simply supported circular plate subjected to dynamic load have been studied at first by Hopkins and Prager (1954). In the past forty years, a number of studies (Jones and Oliveira, 1980; Jones, 1989; Florence, 1977; Symonds and Wierzbicki, 1979) have focused on this subject by introducing various boundary conditions, loading conditions and plastic flow assumptions for circular plate. So far, the above studies are all on the basis of the Tresca yield criterion, namely maximum shear stress yield criterion. Little attention has been paid to investigate the influence of yield criteria on the dynamic plastic behavior of circular plates. In fact, strength envelopes of a great of metal materials are in agreement with the Mises criterion; strength envelopes of some mild steel and aluminum alloy close to the twin shear stress yield criterion (Yu, 1983), or the maximum principal deviatoric stress yield criterion (Hill, 1951). Based on the twin shear stress yield assumption, Yu and He (1991) supposed a unified yield criterion (UYC) by introducing a weighting coefficient in the twin shear stress yield criterion. The Tresca yield criterion is a special case of the UYC, and the Mises yield criterion can be lineally approximated by the UYC. Investigating the dynamic plastic response behavior in view of the UYC has theoretical significance and wide-range applications. The mathematical expression of the UYC is piecewise linear, so it can be conveniently used to perform plastic limit analyses of axisymmetric structures. The authors presented the exact static plastic solutions of simply supported circular plates subjected to partial uniform distributed pressure in view of the UYC (Ma et al., 1995). In this paper, dynamic plastic responses are obtained for circular plate subjected to a uniformly distributed moderate pulse with rectangular pressure-time history. The entire plate is divided into two different regions corresponding to two related yield lines. A series of results in specific conditions of the UYC are derived and compared mutually.

2. Unified yield criterion

Based on orthogonal octahedron of twin shear element model (Yu, 1983), the UYC assumes that materials fail when a certain function of the two bigger principal shear stresses reaches a limit value. The mathematical expression of the UYC is

$$\tau_{13}+b\tau_{12} = C \quad \text{when } \tau_{12} \geqslant \tau_{23} \tag{1a}$$

$$\tau_{13}+b\tau_{23} = C \quad \text{when } \tau_{12} \leqslant \tau_{23} \tag{1b}$$

where τ_{13}, τ_{12} and τ_{23} are principal shear stresses and $\tau_{13} = (\sigma_1-\sigma_3)/2$; $\tau_{12} = (\sigma_1-\sigma_2)/2$; and $\tau_{23} = (\sigma_2-\sigma_3)/2$; σ_1, σ_2 and σ_3 are principal stresses and $\sigma_1 \geqslant \sigma_2 \geqslant \sigma_3$; C is material strength parameter; and b is a weighting coefficient that reflects the influence of the intermediate principal shear stress. Figure 1 shows the projection in deviatoric plane of limit surface of UYC in triaxial stress state. Rewriting (1a, b) in terms of principal stresses, it has

$$\sigma_1 - \frac{1}{1+b}(b\sigma_2+\sigma_3) = \sigma_0 \quad \text{when } \sigma_2 \leqslant \frac{1}{2}(\sigma_1+\sigma_3) \tag{2a}$$

$$\frac{1}{1+b}(\sigma_1+b\sigma_2)-\sigma_3 = \sigma_0 \quad \text{when } \sigma_2 \geqslant \frac{1}{2}(\sigma_1+\sigma_3) \tag{2b}$$

where σ_0 is uniaxial yield strength, b reflects the effect of intermediate principal stress σ_2 on material

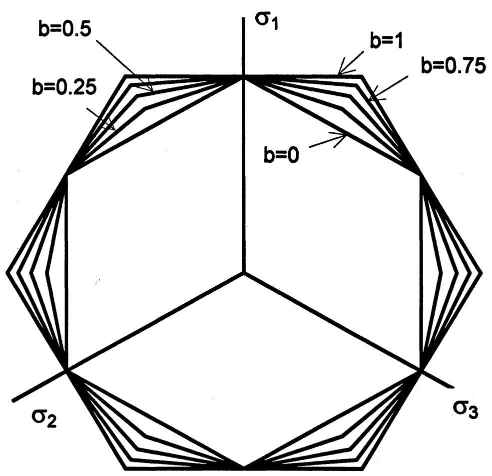

Fig. 1. UYC in deviatoric plane.

strength. When b varies from 0–1, a family of convex yield criteria those are suitable for different kinds of materials are deduced. In particular, it becomes the Tresca criterion when $b = 0$ in the UYC. The maximum principal deviatoric stress criterion or the twin shear stress criterion is obtained when $b = 1$. The Mises criterion can be approximated by the UYC of $b = 0.5$. Expression of the UYC is obviously a piecewise linear function.

3. Dynamic equations and boundary conditions

The simply supported circular plate with radius a and thickness h which is subjected to a partial uniformly distributed transverse load P is assumed that plastic flow of the material obeys the unified yield criterion. Clearly, a rigid, perfectly plastic circular plate accelerates when it is subjected to larger pressures which satisfy the inequality $P \geqslant P_s$, here P_s is the static plastic limit load, if the pressure is released for a short time. The plate reaches an equilibrium position (with a deformed profile) when all the external dynamic energy has been expended as plastic work. It is convenient to divide the subsequent analysis into the two phases $0 \leqslant t \leqslant \tau$; $\tau \leqslant t \leqslant T$ for a moderate impulsive loading, where τ is the duration of pulse and T is the duration of response.

Using the dimensionless variables defined in notation, the governing equations of circular plates are as follows

$$\partial(rm_r)/\partial r - m_\theta - rq = 0 \tag{3}$$

$$\partial(rq)/\partial r + rp - \mu r\ddot{w} = 0 \tag{4}$$

and

$$\dot{k}_r = -\partial^2\dot{w}/\partial r^2, \quad \dot{k}_\theta = -(\partial\dot{w}/\partial r)/r \tag{5a,b}$$

where p is a partial uniformly distributed rectangular load. In the first of motion ($0 \leqslant t \leqslant \tau$), it has

$$p = \begin{cases} p_0 & 0 \leqslant r \leqslant r_p \\ 0 & r_p \leqslant r \leqslant 1 \end{cases} \tag{6}$$

and in the second phase of motion ($\tau \leqslant t \leqslant T$), it becomes

$$p = 0 \tag{7}$$

where r_p is dimensionless loading radius.

The yield condition is controlled by the generalized stresses m_r and m_θ. Figure 2 shows the yield lines of the unified yield criterion in m_θ–m_r space. In plastic limit state, moments of the plate center ($r = 0$) satisfies $m_r = m_\theta = 1$ (point A in Fig. 2), the simply supported edge ($r = 1$) satisfies $m_r = 0$ (point C in Fig. 2). Bending moments of all the points in the plate are located in the sides AB and BC for the normality requirement of plasticity (Drucker's postulate). The yield conditions of AB and BC in Fig. 2 are expressed as follows,

$$m_\theta = a_i m_r + b_i \quad (i = 1, 2) \tag{8}$$

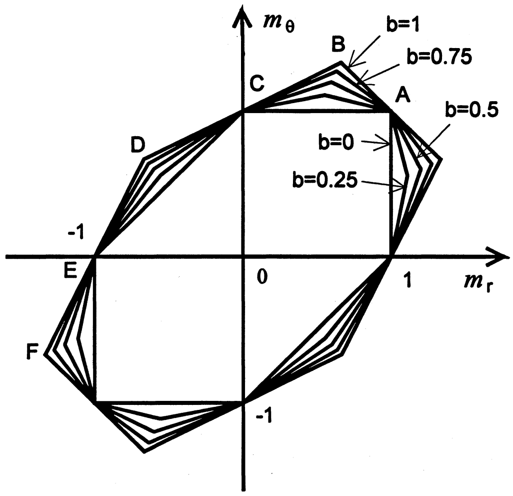

Fig. 2. Unified yield criterion in m_θ–m_r space.

where a_i and b_i are constants, they are $a_1 = -b$, $b_1 = 1+b$, $a_2 = b/1+b$ and $b_2 = 1$ corresponding to the two sides AB ($i = 1$) and BC ($i = 2$).

According to associated flow rule, there are

$$\dot{k}_r = \lambda\, \partial F/\partial m_r, \quad \dot{k}_\theta = \lambda\, \partial F/\partial m_\theta \tag{9}$$

where F in eqn (9) is plastic potential which is the same as the yield function. Thus, the following equation is deduced,

$$\dot{k}_r = -a_i \dot{k}_\theta \tag{10}$$

Equations (3) and (4) with the aid of eqn (8) give the moment governing equation as follows

$$\partial^2 (rm_r)/\partial r^2 - a_i\, \partial m_r/\partial r = -rp + \mu r \ddot{w} \tag{11}$$

Governing equation of the transverse velocity is derived as the following by substituting eqn (5a, b) into eqn (10)

$$\partial^2 \dot{w}/\partial r^2 + a_i\, \partial \dot{w}/(r\, \partial r) = 0 \tag{12}$$

4. First phase of motion ($0 \leqslant t \leqslant \tau$)

In the first phase of motion, the plate is subjected to a constant loading p_0 in the inner region $0 \leqslant r \leqslant r_p$. Integrating eqn (12) twice with respect to r predicts the transverse velocity corresponding to the two sides as follows

$$\dot{w} = \dot{w}_1 \begin{cases} c_{11} r^{1-a_1} + c_{21} & 0 \leqslant r \leqslant r_1 \\ c_{12} r^{1-a_2} + c_{22} & r_1 \leqslant r \leqslant 1 \end{cases} \tag{13}$$

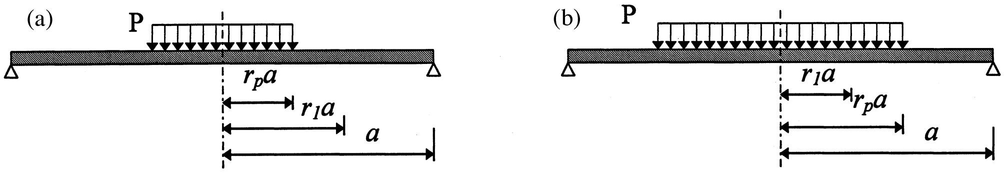

Fig. 3. (a) Case 1 $r_p \leqslant r_1$; (b) Case 2 $r_p \geqslant r_1$.

where, c_{1i}, c_{2i} $(i = 1, 2)$ are integral constants; r_1 is the dividing radius where the moments are locating at point B in Fig. 2; $\dot{w}_1$ is the velocity response of the plate center which is a function of time t. Continuity and boundary conditions of velocity are (1) $\dot{w}(r = 0) = \dot{w}_1$; (2) $\dot{w}(r = r_1)$ and $\mathrm{d}\dot{w}/\mathrm{d}r(r = r_1)$ are continuous; and (3) $\dot{w}(r = 1) = 0$. Considering these conditions, the constants c_{1i} and c_{2i} in eqn (13) are then derived as,

$$c_{11} = -\frac{r_1^{-b(2+b)(1+b)}}{(1+b)^2-(2b+b^2)r_1^{1/(1+b)}}, \quad c_{21} = 1 \quad \text{and}$$

$$c_{12} = -c_{22} = -\frac{(1+b)^2}{(1+b)^2-(2b+b^2)r_1^{1/(1+b)}}$$

There are two cases of moment response during the first phase of motion as shown, respectively, in Fig. 3a and b. For both the two cases, the boundary conditions and continuity conditions of radial moment are: (4) $m_r(r = 0) = 1$; (5) $m_r(r = r_1)$ is continuous, and equals $(1+b)/(2+b)$; (6) $\partial m_r/\partial r(r = r_1)$ is continuous; (7) $m_r(r = r_p)$ is continuous; (8) $\partial m_r/\partial r(r = r_p)$ is continuous; and (9) $m_r(r = 1) = 0$. The conditions (6) and (8) are deduced from the continuity of shear force q in eqn (3) with the aid of continuity of m_r and m_θ.

4.1. *Case* 1 ($\mathrm{r_p} \leqslant \mathrm{r_1}$)

For the first case, that the plate is subjected to a rectangular impulsive loading p_0 with $r_p \leqslant r_1$, the moment response field is derived by integrating eqn (11) twice with respect to r as follows

$$m_{r1} = \frac{-p_0+\mu\ddot{w}_1 c_{21}}{2(3-a_1)}r^2 + \frac{\mu\ddot{w}_1 c_{11}}{(3-a_1)(4-2a_1)}r^{3-a_1} + c_{31}r^{-1+a_1} + c_{41} \quad 0 \leqslant r \leqslant r_p \tag{14a}$$

$$m_{r2} = \frac{\mu\ddot{w}_1 c_{21}}{2(3-a_1)}r^2 + \frac{\mu\ddot{w}_1 c_{11}}{(3-a_1)(4-2a_1)}r^{3-a_1} + c_{32}r^{-1+a_1} + c_{42} \quad r_p \leqslant r \leqslant r_1 \tag{14b}$$

$$m_{r3} = \frac{\mu\ddot{w}_1 c_{22}}{2(3-a_2)}r^2 + \frac{\mu\ddot{w}_1 c_{12}}{(3-a_2)(4-2a_2)}r^{3-a_2} + c_{33}r^{-1+a_2} + c_{43} \quad r_1 \leqslant r \leqslant 1 \tag{14c}$$

where c_{3i}, c_{4i} $(i = 1, 2, 3)$ are integral constants and they are derived from the continuity and boundary conditions (4)–(9) as

$$c_{31} = 0, \quad c_{41} = 1, \quad c_{32} = \frac{p_0 r_p^{3-a_1}}{(1-a_1)(3-a_1)}, \quad c_{42} = 1-\frac{p_0 r_p^2}{2(1-a_1)}$$

$$c_{33} = \left[-\frac{1+b}{2+b} - \frac{\mu\ddot{w}_1 c_{22}}{2(3-a_2)}(1-r_1^2) - \frac{\mu\ddot{w}_1 c_{12}}{(3-a_2)(4-2a_2)}(1-r_1^{3-a_2}) \right] \Big/ (1-r_1^{-1+a_2})$$

$$c_{43} = \left[-\frac{1+b}{2+b} r_1^{1-a_2} - \frac{\mu\ddot{w}_1 c_{22}}{2(3-a_2)}(1-r_1^{3-a_2}) - \frac{\mu\ddot{w}_1 c_{12}}{(3-a_2)(4-2a_2)}(1-r_1^{4-2a_2}) \right] \Big/ (1-r_1^{1-a_2})$$

as well as

$$\mu\ddot{w}_1 = \frac{(3-a_1)(4-2a_1)}{(2-a_1)r_1^2 + c_{11} r_1^{3-a_1}} \left[-\frac{1}{2+b} + \frac{p_0 r_p^2}{2(1-a_1)} - \frac{p_0 r_p^{3-a_1}}{(1-a_1)(3-a_1)} r_1^{-1+a_1} \right] \tag{15}$$

and the dividing radius r_1 satisfies

$$\mu\ddot{w}_1 \left(\frac{1}{3-a_1} - \frac{c_{22}}{3-a_2} \right) + \mu\ddot{w}_1 \left(\frac{c_{11} r_1^{2-a_1}}{4-2a_1} - \frac{c_{12} r_1^{2-a_2}}{4-2a_2} \right)$$
$$+ (a_1-1)c_{32} r_1^{-2+a_1} - (a_2-1)c_{33} r_1^{-2+a_2} = 0 \tag{16}$$

For given rectangular impulsive loading p_0 and loading bearing radius r_p, r_1 can be calculated from eqn (16) by half interval search in the range of $(r_p, 1)$ with the aid of eqn (15) and the expression of all the integral constants.

4.2. *Case* 2 ($r_p \geqslant r_1$)

When the loading radius is larger with inequality $r_p \geqslant r_1$, it leads to Case 2. The moment distribution is expressed as follows by integrating eqn (11) twice again

$$m_{r1} = \frac{-p_0 + \mu\ddot{w}_1 c_{21}}{2(3-a_1)} r^2 + \frac{\mu\ddot{w}_1 c_{11}}{(3-a_1)(4-2a_1)} r^{3-a_1} + c_{31} r^{-1+a_1} + c_{41} \quad 0 \leqslant r \leqslant r_1 \tag{17a}$$

$$m_{r2} = \frac{-p_0 + \mu\ddot{w}_1 c_{22}}{2(3-a_2)} r^2 + \frac{\mu\ddot{w}_1 c_{12}}{(3-a_2)(4-2a_2)} r^{3-a_2} + c_{32} r^{-1+a_2} + c_{42} \quad r_1 \leqslant r \leqslant r_p \tag{17b}$$

$$m_{r3} = \frac{\mu\ddot{w}_1 c_{22}}{2(3-a_2)} r^2 + \frac{\mu\ddot{w}_1 c_{12}}{(3-a_2)(4-2a_2)} r^{3-a_2} + c_{33} r^{-1+a_2} + c_{43} \quad r_p \leqslant r \leqslant 1 \tag{17c}$$

According to the boundary conditions and continuous conditions (4)–(9), the integral constants are rewritten as

$$c_{31} = 0, \quad c_{41} = 1$$

$$c_{42} = \frac{b_2}{1-a_2} + \frac{1}{2}\frac{\mu\ddot{w}_1}{1-a_2}(c_{22}-c_{21})r_1^2 - \frac{\mu\ddot{w}_1}{1-a_2}\left(\frac{c_{12} r_1^{3-a_2}}{3-a_2} - \frac{c_{11} r_1^{3-a_1}}{3-a_1} \right)$$

$$c_{32} = \left[\frac{1+b}{2+b} - c_{42} - \frac{-p_0 + \mu\ddot{w}_1 c_{22}}{2(3-a_2)} r_1^2 - \frac{\mu\ddot{w}_1 c_{12}}{(3-a_2)(4-2a_2)} r_1^{3-a_2} \right] \Big/ r_1^{-1+a_2}$$

$$c_{33} = \frac{p_0 r_p^{3-a_2}}{(1-a_2)(3-a_2)} + c_{32}, \quad c_{43} = c_{42} + c_{32} r_p^{-1+a_2} - \frac{p_0 r_p^2}{2(3-a_2)} - c_{33} r_p^{-1-a_2}$$

as well as

$$\mu \ddot{w}_1 = \frac{(2+b)p_0 r_1^2 - 2(3+b)}{(2+b)r_1^2 + c_{11} r_1^{3+b}} \tag{18}$$

and r_1 satisfies

$$\frac{\mu \ddot{w}_1 c_{22}}{2(2-a_2)} + \frac{\mu \ddot{w}_1 c_{12}}{(3-a_2)(4-2a_2)} + c_{33} + c_{43} = 0 \tag{19}$$

The dividing radius r_1 in the eqn (19) is calculated similar to eqn (16) by using half interval search in the range of $(0, r_p)$. The moment fields of Case 2 are then determined after substituting r_1 back into all the integral constants and eqns (17) and (18).

For a given impulsive load P which satisfies the static and kinematic admissibility, there is a critical state between the two cases shown, respectively, in Fig. 3a and b. The critical dividing radius r_{1p} is obtained from the particular case of $r_{1p} = r_p = r_1$. Then, if the actual loading radius is less than the critical dividing radius r_{1p}, the moment response fields are calculated using Case 1. If not then using Case 2.

Equations (16) and (18) show that $\ddot{w}_1$ is a constant during the first phase of motion. The transverse displacement and velocity at the end of the phase of motion for both cases are,

$$w = \ddot{w}_1 \tau^2 (c_{1i} r^{1-a_i} + c_{2i})/2 \quad (i = 1, 2) \tag{20}$$

and

$$\dot{w} = \ddot{w}_1 \tau (c_{1i} r^{1-a_i} + c_{2i})/2 \quad (i = 1, 2) \tag{21}$$

respectively. Equation (21) leads to a kinetic energy

$$k_e = \pi \mu M_0 a \ddot{w}_1^2 \tau^2 K \tag{22}$$

where

$$K = \frac{(c_{11})^2}{4-2a_1} r_1^{4-2a_1} + \frac{2c_{11}c_{21}}{3-a_1} r_1^{3-a_1} + \frac{(c_{21})^2}{2} r_1^2 + \frac{(c_{12})^2}{4-2a_2}(1 - r_1^{4-2a_2}) + \frac{2c_{12}c_{22}}{3-a_2}(1 - r_1^{3-a_2}) + \frac{(c_{22})^2}{2}(1 - r_1^2)$$

which is dissipated plastically during the second phase of motion

5. Second phase of motion ($\tau \leqslant t \leqslant T$)

The circular plate is unloaded during this phase of motion and, therefore $p = 0$ on the whole plate. But plastic deformation continues in order to dissipate the kinetic energy present in the plate at $t = \tau$. The transverse velocity profile during this phase of motion has the same form as eqn (13) of the first phase of motion except the dividing radius r_1 is replaced by r_2. Identical to the first phase of motion, the moment response field is again obtained as

$$m_{r1} = \frac{\mu\ddot{w}_2 c_{21}}{2(3-a_1)} r^2 + \frac{\mu\ddot{w}_2 c_{11}}{(3-a_1)(4-2a_1)} r^{3-a_1} + c_{31} r^{-1+a_1} + c_{41} \quad 0 \leqslant r \leqslant r_2 \tag{23a}$$

$$m_{r2} = \frac{\mu\ddot{w}_2 c_{22}}{2(3-a_2)} r^2 + \frac{\mu\ddot{w}_2 c_{12}}{(3-a_2)(4-2a_2)} r^{3-a_2} + c_{32} r^{-1+a_2} + c_{42} \quad r_2 \leqslant r \leqslant 1 \tag{23b}$$

The boundary and continuity conditions to (10) $m_r(r = 0) = 1$; (11) $m_r(r = r_2)$ is continuous, and equals $(1+b)/(2+b)$; (12) $\partial m_r/\partial r(r = r_2)$ is continuous; and (13) $m_r(r = 1) = 1$. Thus, the integral constants are calculated again as

$$c_{31} = 0, \quad c_{41} = 1$$

$$c_{32} = \left[-\frac{1+b}{2+b} - \frac{\mu\ddot{w}_2 c_{22}}{2(3-a_2)}(1-r_2^2) - \frac{\mu\ddot{w}_2 c_{12}}{(3-a_2)(4-2a_2)}(1-r_2^{3-a_2}) \right] \bigg/ (1-r_2^{-1+a_2})$$

$$c_{42} = \left[-\frac{1+b}{2+b} r_2^{1-a_2} - \frac{\mu\ddot{w}_2 c_{22}}{2(3-a_2)}(1-r_2^{3-a_2}) - \frac{\mu\ddot{w}_2 c_{12}}{(3-a_2)(4-2a_2)}(1-r_2^{4-2a_2}) \right] \bigg/ (1-r_2^{1-a_2})$$

as well as

$$\mu\ddot{w}_2 = \frac{-2(3+b)}{(2+b)r_2^2 + c_{11} r_2^{3+b}} \tag{24}$$

and r_2 satisfy

$$\frac{\mu\ddot{w}_2 c_{22}}{2(3-a_2)} + \frac{\mu\ddot{w}_2 c_{12}}{(3-a_2)(4-2a_2)} + c_{33} + c_{43} = 0 \tag{25}$$

where $\mu\ddot{w}_2$ remains constant during the second phase of motion.

A straight integration of eqn (24) with respect to time predicts the transverse displacement at the plate center

$$w_2 = \tfrac{1}{2}\ddot{w}_2(t-\tau)^2 + \tfrac{1}{2}\ddot{w}_1\tau(2t-\tau) \tag{26}$$

when eliminating the two constants of integration by ensuring continuity with the transverse displacement and velocity at the end of the first phase of motion ($t = \tau$). $\ddot{w}_1$ and $\ddot{w}_2$ defined by eqns (15) and (24), respectively, are independent on time. Equation (26) gives $\dot{w}_2 = 0$ when $t = T$, where

$$T = \eta\tau \tag{27}$$

T is the total duration of response and η is the response time factor defined as follows,

$$\eta = 1 - \ddot{w}_1/\ddot{w}_2 \tag{28}$$

The associated permanently deformed transverse displacement profile is

$$W_f = -\tfrac{1}{2}\ddot{w}_2\tau^2\eta(\eta-1)(c_{1i}r^{1-a_i}+c_{2i}), \quad i = 1,2 \tag{29}$$

6. Static and kinematic admissibility

When the impulsive time τ is long enough and the transverse response acceleration $\ddot{w}_1$ during the first phase of motion is equal to 0, the dynamic solutions degenerate to static plastic limit solutions for the entire plate in plastic state. The static limit loads are derived from eqns (15) or (18) as

$$p_s = \frac{2(1+b)(3+b)}{(2+b)[(3+b)-2(r_p/r_s)^{1+b}]r_p^2} \tag{30}$$

or

$$p_s = \frac{6+2b}{(2+b)r_s^2} \tag{31}$$

respectively, for the two cases shown in Fig. 3a and b. Where p_s is the static plastic limit load; r_s is the dividing radius which divide the plate into two parts with the moment profiles responding to the two lines AB and BC in Fig. 2. r_s calculated from eqn (16) or eqn (19) with the aid of $\mu\ddot{w}_1 = 0$ and eqns (30) and (31). The critical dividing radius in static plastic limit state satisfying $r_{sp} = r_p = r_s$ is equal to $2^{-(1+b)}$ which has been examined in reference (Ma et al., 1995).

The circular plate can be subjected to a short duration pressure that exceeds the static plastic limit loading, but it is necessary to demonstrate that the foregoing theoretical solutions do not violate the yield condition and are, therefore, statically admissible. The radial moment field is a decrease function according to the yield condition in Fig. 2. In order to avoid a yield violation at $r = 0$ and $r = 1$ in the bending moment distribution, it is necessary to ensure

$$\partial m_r/\partial r \leqslant 0, \quad \partial^2 m_r/\partial r^2 \leqslant 0 \quad \text{at } r = 0 \tag{32}$$

$$\partial m_r/\partial r \leqslant 0, \quad \partial^2 m_r/\partial r^2 \geqslant 0 \quad \text{at } r = 1 \tag{33}$$

For the first phase of motion, $\partial m_r/\partial r(r = 0) = 0$ is satisfied automatically at the plate center, thus it needs only to check $\partial^2 m_r/\partial r^2 \leqslant 0$. Differentiating eqn (14a) or (17a) twice with respect to r, the static admissible dynamic load should satisfy

$$p_0+\mu\ddot{w}_1 \leqslant 0 \tag{34}$$

which predicts the maximum dynamic impulsive loading p_{d1} with the aid of eqns (15) and (16) or eqns (18) and (19) for the two cases, respectively. Meanwhile, $\partial m_r/\partial r = 0$ at $r = 1$ predicts another maximum static admissible impulsive load p_{d2} since $\partial^2 m_r/\partial r^2 \geqslant 0$ is satisfied automatically. Thus,

$$\frac{\mu\ddot{w}_1 c_{22}}{3-a_2}+\frac{\mu\ddot{w}_1 c_{12}}{4(2-a_2)}+(-1+a_2)c_{33} = 0 \tag{35}$$

according to eqns (14c) or (17c). p_{d2} is calculated from eqns (15) and (16) or (18) and (19), respectively, for the two cases with the aid of eqn (35). The radial bending moment distribution during the second phase of motion from eqn (23) is independent of p_0 and time and is statically admissible. Thus the static admissible load needs to satisfy the inequality,

$$p_s \leqslant p_0 \leqslant p_d = \min(p_{d1}, p_{d2}) \tag{36}$$

or

$$1 \leqslant \alpha \leqslant \alpha_d \tag{37}$$

where p_d is maximum statically admissible impulsive loading, α and α_d are defined as statically admissible loading factor and maximum statically admissible loading factor, respectively, and

$$\alpha = p_0/p_s; \quad \alpha_d = p_d/p_s \tag{38}$$

The response acceleration during either the first phase of motion or the second phase of motion is independent to time and the displacement, velocity and acceleration on the entire plate are continuous during the entire response time, so the dynamic solutions are obviously kinematically admissible. The theoretical analysis above with $1 \leqslant \alpha \leqslant \alpha_d$ is statically admissible while the associated transverse velocity fields are kinematically admissible. Thus, the solution is exact throughout the entire response of a rigid, perfectly plastic circular plate.

The moment distributions will violate the yield condition when the impulsive loading P increases to $\alpha \geqslant \alpha_d$. In order to avoid this violation, it is convenient to suppose that the moment profiles are distributed as shown in Fig. 5a and b corresponding to the two violating cases plotted, respectively, in Fig. 4a and b. The velocity profiles remain as decreasing function; however, the acceleration responses are not constant and the plastic hinge moves during the response time. The dynamic solution for the plate under intense impulsive load should be analyzed by numerical method, which will be examined in the future.

7. Analysis results

The foregoing solutions predict maximum transverse displacement response and minimum statically admissible impulsive load with respect to the Tresca criterion ($b = 0$), minimum trans-

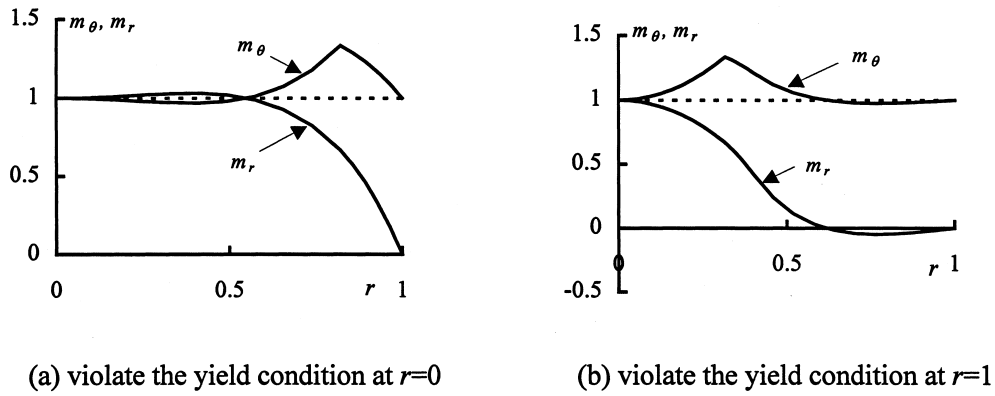

Fig. 4. Statically inadmissible moment profiles: (a) violate the yield condition at $r = 0$; (b) violate the yield condition at $r = 1$.

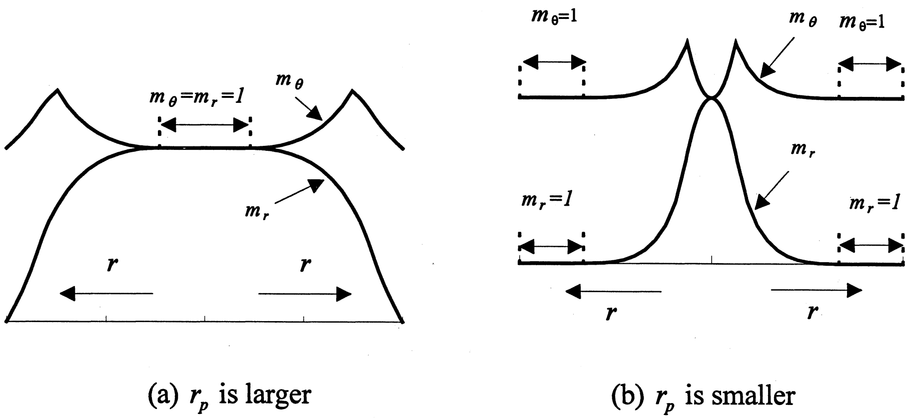

Fig. 5. Moment profiles of intense loading: (a) r_p is larger, (b) r_p is smaller.

verse displacement response and maximum statically admissible impulsive load with respect to the twin shear stress criterion ($b = 1$), respectively. Solutions of the Mises criterion are between those obeying the Tresca criterion and the twin shear stress criterion, and can be approximated by the special case of the UYC when $b = 0.5$. For a given impulse loading radius r_p and the pulse force p_0 satisfying statically admissibility, r_1 and r_2 locating in the range of $(0, 1)$ are calculated from eqns (16) or (19) for the first phase of motion and eqn (25) for the second phase of motion, respectively. Substituting r_1 and r_2 into all the integration constants and corresponding equations, moment response fields, velocity response fields and displacement response fields of the plate are then defined for the two motion phases.

Figure 6a and b show the moment fields during the first phase of motion when the plate is subjected by a uniformly impulsive load ($r_p = 1$) with respect to the three special cases of yield criterion, with the load factor $\alpha = 1$ and $\alpha = \alpha_d$, respectively. Figure 7 shows the moment fields during the second phase of motion which is independent of the loading radius r_p and loading factor α. Figures 8–10 illustrate the permanently deformed transverse displacements, displacement responses and velocity responses of the plate center for the three special criterion when $r_p = 1$ and $\alpha = \alpha_d$.

Figures 11a, b and 12, show the moment profiles, velocity profiles during the first phase of motion and the permanently deformed transverse displacements when the plate is subjected to a concentrated impulsive load with $r_p = 0.01$. The moment fields are singular at the plate center because the shear force at the center is infinite. The statically admissible impulsive load p_d is close to the static plastic limit load p_s, thus we need to apply the assumption shown in Fig. 5b for a fully rigid-plastic circular plate subjected to concentrated load. It has been proved that the total static plastic limit load $P_T = \pi r_p^2 Pa^2$ for concentrated load satisfies $P_T = 2\pi M_0$ no matter what the weighting parameter b is selected (Ma et al., 1995), although the moment fields and velocity fields are quite different with different yield criteria.

The profile of deformed transverse displacement restore to the profile similar to the case of fully uniformly distributed load since the dividing radius r_2 during the second phase of motion is independent of loading radius r_p. The unified yield criterion, besides the special case of the Tresca

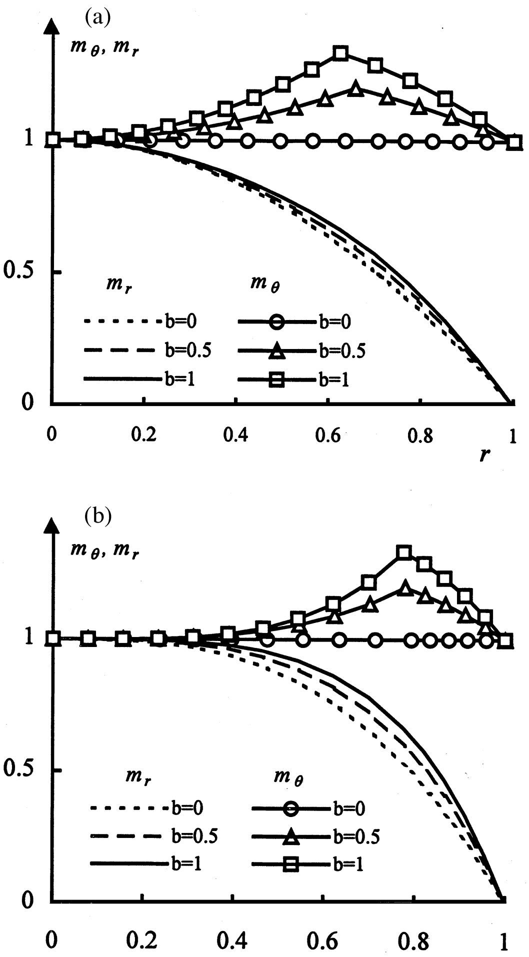

Fig. 6. (a) Moment fields during the first phase of motion ($\alpha = 1$). (b) Moment fields during the first phase of motion ($\alpha = \alpha_d$).

criterion, leads to smooth velocity distribution at the plate center; meanwhile, the velocity profile varies depending on the loading radius r_p. The Tresca criterion as a special case of the unified yield criterion leads to linear velocity profiles and there is singularity at the plate center for velocity fields, in spite of r_p.

Relation of the maximum statically admissible loading factor α_d to loading radius r_p is plotted in Fig. 13, which shows clearly the two loading action regions corresponding to the two statically admissibility shown in Fig. 4a and b with respect to the three yield criteria. Relation of response delaying time factor η has a very close outline to Fig. 13 as shown in Fig. 14; however, they completely overlap when the Tresca criterion is used. It leads to $\alpha_d = 2$ and $\eta = 2$ for the case of fully uniformly distributed impulsive load, when $b = 0$, which is the same as the results examined by Hopkins and Prager (1954).

Figure 15 demonstrates that the effect of yield criteria to the dynamic solution is greater than

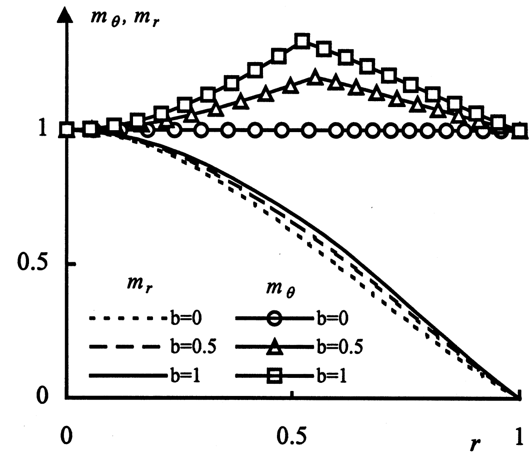

Fig. 7. Moment fields during the second phase of motion.

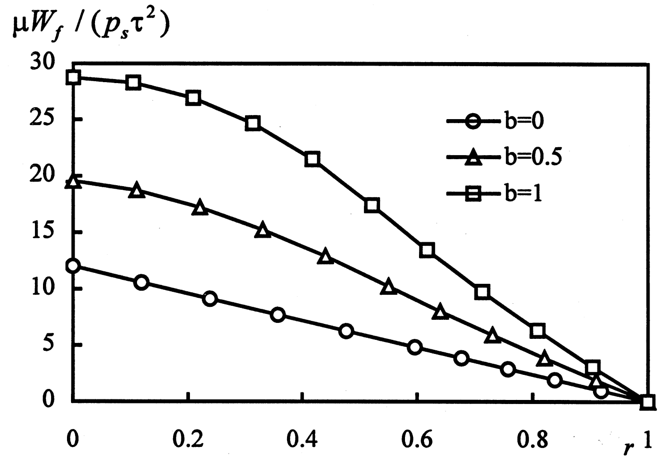

Fig. 8. Permanently deformed transverse displacements ($r_p = 1, \alpha = \alpha_d$).

that to static plastic limit state. Figure 16 shows that the Tresca criterion estimates the maximum permanent transverse displacement, which has been proved greater than the experimental results (Jones, 1989).

8. Conclusions

Unified yield criterion with piecewise linear mathematical expression are applied successfully to analyze the dynamic response behavior for simply supported circular plate under moderate impulsive load. A series of analytical results are illustrated to show the effects of yield criteria to dynamic behavior of the plate. Particularly, the results show, the Tresca criterion ($b = 0$) leads to maximum

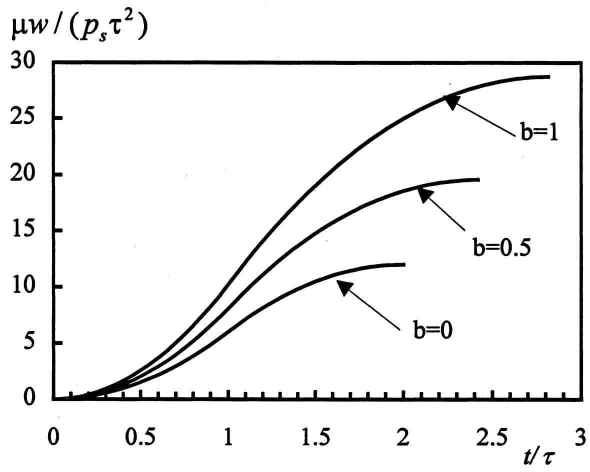

Fig. 9. Displacement responses at the plate center ($r_p = 1, \alpha = \alpha_d$).

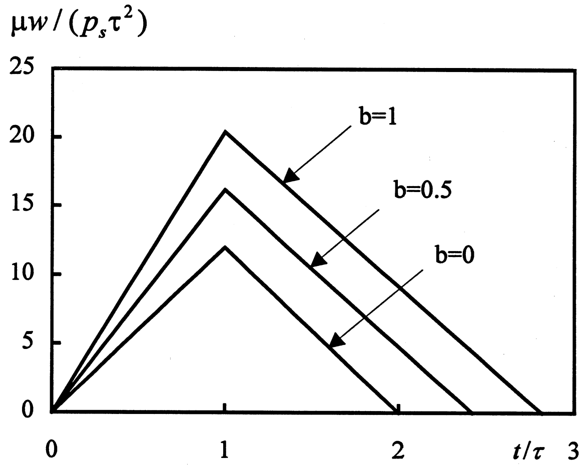

Fig. 10. Velocity responses at the plate center ($r_p = 1, \alpha = \alpha_d$).

transverse displacement response and minimum statically admissible impulsive load. While the twin shear stress criterion predicting the minimum transverse displacement response and maximum statically admissible impulsive loading. Solution of the Mises criterion are approximated by the linear function of the UYC with $b = 0.5$. This paper clearly illustrated the influences of yield criteria on the dynamic behavior of the plate. It shows that the influences are greater for the plate in dynamic plastic limit state than in static plastic limit state.

The solutions of this paper have theoretical meaning and more wider application range. By choosing a certain material parameter, the unified yield criterion can be applied to all the isotropic metal materials. The authors suggested two types of moment profiles when the plate is subjected to partial uniformly distributed intense impulsive load, which will be presented in the future.

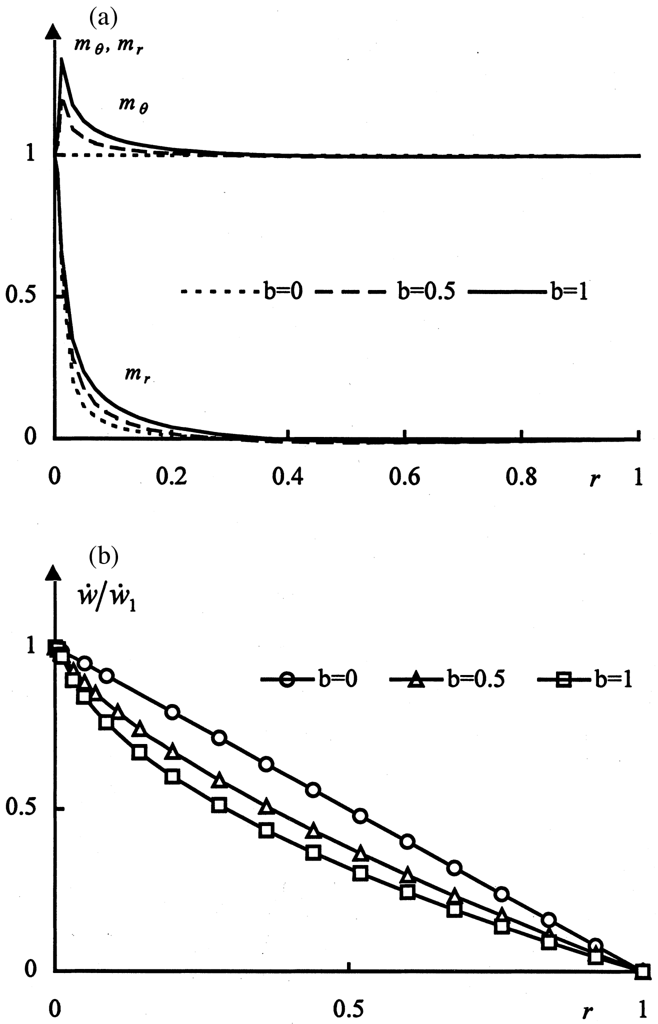

Fig. 11. (a) Moment profiles of the first phase of motion ($\alpha = \alpha_d, r_d = 0.01$). (b) Velocity profiles of the first phase of motion ($\alpha = \alpha_d, r_d = 0.01$).

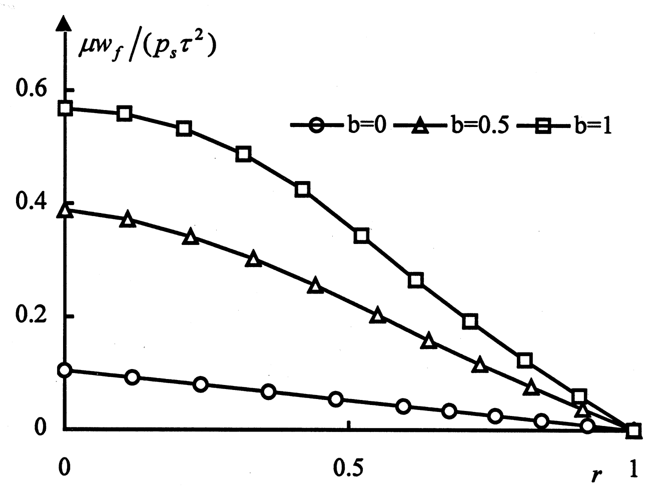

Fig. 12. Permanently deformed transverse displacement ($\alpha = \alpha_d, r_p = 0.01$).

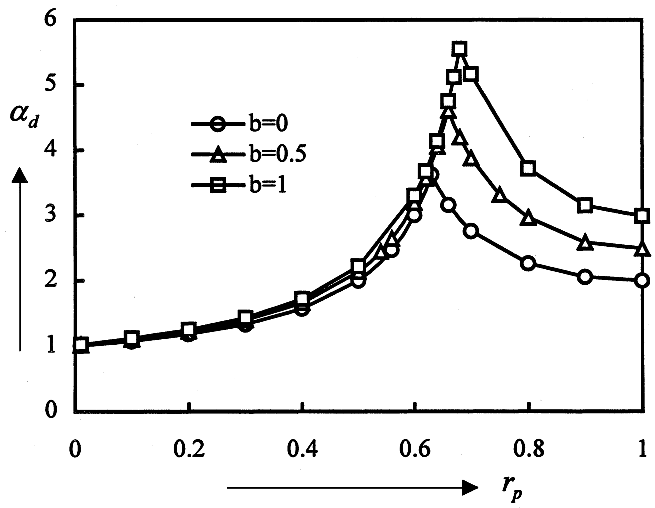

Fig. 13. Curves of α_d to r_p.

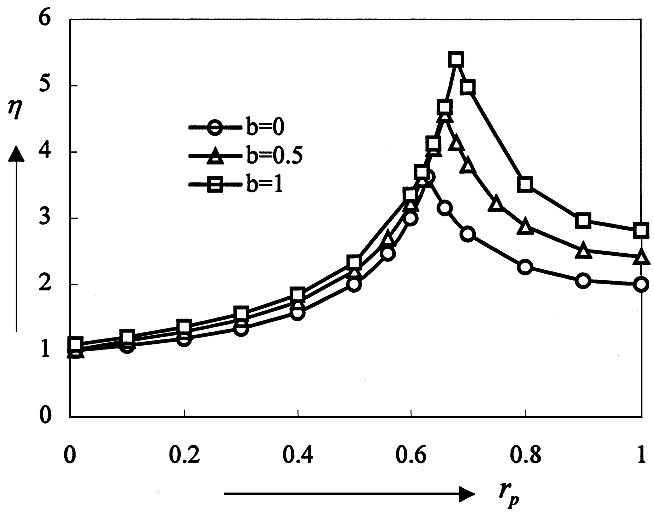

Fig. 14. Curves of η to r_p.

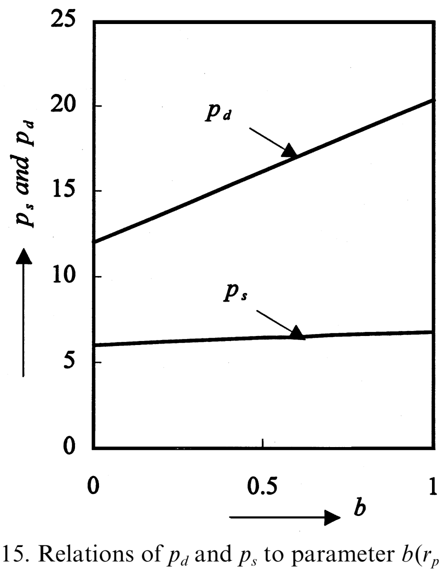

Fig. 15. Relations of p_d and p_s to parameter $b(r_p = 1)$.

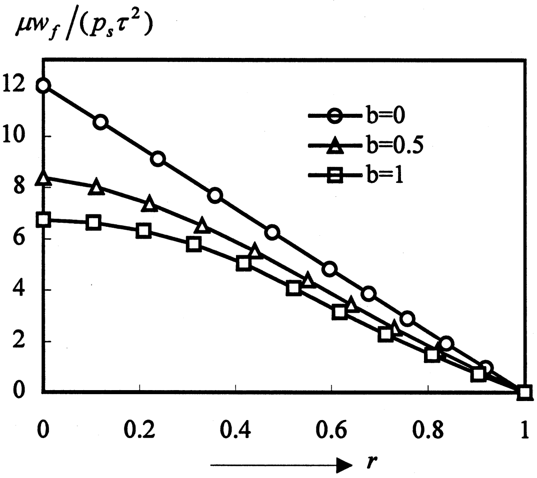

Fig. 16. Permanently deformed transverse displacement ($r_p = 1, p_0 = 12$).

References

Florence, A.L., 1977. Response of circular plates to central pulse loading. International Journal of Solids and Structures 13, 1091–1102.

Hopkins, H.G., Prager, W., 1954. On the dynamics of plastic circular plates. Journal of Applied Mathematics and Physics (ZAMP) 5, 317–330.

Jones, N., 1989. Structural Impact. Cambridge University Press.

Jones, N., De Oliveira, J.G., 1980. Dynamic plastic response of circular plates with transverse shear and rotatory inertia. Journal of Applied Mechanics 47 (1), 27–34.

Ma, G.W., Yu, M.H., Iwasaki, S., Miyamoto, Y., Deto, H., 1995. Unified plastic limit solution to circular plate under portion uniform loading. Journal of Structural Engineering, JSCE 41A, 385–392.

Stronge, W.J., Yu, T.X., 1993. Dynamic Models for Structural Plasticity. Springer-Verlag, London.

Symonds, P.S., Wierzbicki, T., 1979. Membrane mode solutions for impulsively loaded circular plates. Journal of Applied Mechanics 46 (1), 58–64.

Yu, M.H., 1983. Twin shear stress yield criterion. International Journal of Mechanical Science 25 (1), 71–74.

Yu, M.H., He, L.N., 1991. A new model and theory on yield and failure of materials under complex stress state. In: Mechanical Behavior of Materials-6, vol. 3. Pergamon Press, pp. 841–846.